A semi-analytical solution for consolidation around a spherical cavity in an elasto-perfectly plastic medium and its potential application for tunnelling

[1]Ashraf S. Osman, [2]M. Rouainia

[1]School of Engineering, Durham University, South Road, Durham DH1 3LE, UK

[2]School of Civil Engineering and Geosciences, Newcastle University, Newcastle, NE 17U, U.K

Abstract

An analytical solution for consolidation around spherical cavity contraction is developed. This solution has the potential to be applied to evaluate consolidation around tunnel heads. The initial excess pore water pressure immediately after the creation of the cavity is evaluated from the cavity expansion/contraction theory using a linear-elastic-perfectly-plastic soil model. Expressions for the decay of pore water pressure with time are obtained using elasticity. Curves shows the variation of pore water pressure with time is plotted in non-dimensional form.

Keywords:
Cavity contraction
Analytical solution
Elasto-plasticity
Consolidation
Tunnel

1 Introduction

Consolidation around a contracting cavity can be applied to the analysis of a variety of geotechnical problems. In pressuremeter tests, for example, the removal of cavity pressure takes place after a partly plastic state of soil has been reached. The interpretation of the test relies on the use of the contracting phase. Yu and Houlsby (1995) obtained closed from solutions for stresses and displacements in the contracting phase of the pressuremeter in-situ test. The solution is based on contraction of spherical cavity in a soil which obeys non-associated Mohr-Column failure criteria. Yu and Rowe (1999) extended this solution to tunnel problems in conjunction with critical state soil models. In tunnel construction in clay, significant change of excess pore water pressure will occur during the construction in response of the reduction of the total stress acting across the tunnel heading. Mair and Taylor (1993) studied the displacement and the excess pore water pressure around different tunnels constructed in London clay and demonstrated that tunnel in saturated clay can be idealised as a cavity contraction problem. They illustrated that displacements and excess pore water pressure during construction can be reasonably predicted by cavity theory assuming the soil is linear perfectly plastic material. The conditions around the tunnels can be simulated by cylindrical cavity and around tunnel heads can be simulated by spherical cavity.

However, once construction is completed or temporarily stopped, the excess pore water suctions will gradually dissipate and the soil surrounding the tunnel will swell and soften. Thus, soil strength will reduce. Therefore, it is important to study the consolidation process around spherical and cylindrical cavity contractions. Consolidation around cylindrical and spherical cavity was studied by many researchers. Consolidation around spherical cavity was first examined by de Josselin de Jong (1953) who studied the pore pressure meters. Cryer (1963) developed a solution for a poroelastic sphere subjected to an external radial stress field in the presence of boundary drainage. Scott (1990) studied the problem of radial compression of a sphere in phase-change soil. Zhou et al., (1998) analyse coupled, linear thermoporoelastic fields in a saturated porous medium under radial and spherical symmetry. Randolph and Wroth (1978) studied the consolidation around a driven pile and Carter (1988) investigated the effect of swelling around boreholes. The problems of consolidation around driven piles and around boreholes are idealised as consolidation around cylindrical cavity and the initial excess pore water pressure immediately after the creation of the cavity is evaluated from the cavity expansion/contraction theory using a linear-elastic-perfectly-plastic soil model.

The aim of this paper is to present an analytical solution around a contracting cavity. In this solution, it is assumed that the distribution of excess pore water pressure immediately after removal of the cavity pressure can be obtained from the undrained analysis of spherical contraction in a linear-elastic perfectly plastic material that obeys Tresca yield criteria. It is also assumed that during the consequent consolidation process the soil skeleton deforms elastically and governs by Darcy's law.

2 Initial excess pore water pressure around contracting spherical cavity

Immediately after creation of the spherical cavity, a plastic zone will be developed adjacent to the cavity (see Fig. 1). In this zone, the equilibrium equation in terms of total stress is governed by:

$$\frac{\partial \sigma_r}{\partial r} + 2\frac{(\sigma_r - \sigma_\theta)}{r} = 0 \tag{1}$$

where σ_r, σ_θ are the circumferential stress and the radial stress respectively, and r represents the radial distance. In undrained conditions:

$$\sigma_\theta - \sigma_r = 2s_u \tag{2}$$

where s_u represents the undrained shear strength. Substituting Eq. (2) into Eq. (1) and making use of $\sigma_r = \sigma_{li}$ at $r = r_o$, together with some algebraic manipulation, the following explicit expression for the radial stress in the plastic zone is obtained:

$$\sigma_r = \sigma_{li} + 4s_u \ln\left(\frac{r}{r_0}\right) \tag{3}$$

and the circumferential stress is given by:

$$\sigma_\theta = \sigma_{li} + 4s_u \ln\left(\frac{r}{r_0}\right) + 2s_u \tag{4}$$

If the initial mean stress before the creation of the spherical cavity is taken to be equal to σ_0, then the change of the total mean stress, Δp, is given by:

$$\Delta p = \frac{(\sigma_r + 2\sigma_\theta)}{3} - \sigma_0 = \sigma_{li} + 4s_u \ln\left(\frac{r}{r_0}\right) + \frac{4}{3}s_u - \sigma_0 \tag{5}$$

Since Δp is equal to zero in the elastic zone, the following relationship is obtained:

$$\Delta\sigma_r = -2\Delta\sigma_\theta \tag{6}$$

when r is equal to r_p, we get the following relationship:

$$\Delta\sigma_\theta - \Delta\sigma_r = 2s_u \tag{7}$$

Combining Eq. (6) and (7) gives:

$$\sigma_r = \sigma_0 - \frac{4}{3}s_u \qquad \text{at } r = r_p \tag{8}$$

where the radius of the plastic zone, r_p, can be evaluated by Eqs. (3) and (8)

$$r_p = r_0 \exp\left(\frac{N}{4} - \frac{1}{3}\right) \tag{9}$$

where N is the stability number defined as follows:

$$N = \frac{\sigma_0 - \sigma_{il}}{s_u} \tag{10}$$

If it is assumed that no consolidation takes place during cavity unloading and the change in mean total stress, Δp, is equal to the excess pore water pressure generated during yielding, the excess pore water pressure distribution around the spherical cavity is given by:

$$\begin{aligned} \frac{u_0}{s_u} &= \frac{4}{3} - N + 4\ln\left(\frac{r}{r_0}\right) && \text{at } r \le r_p \\ \frac{u_0}{s_u} &= 0 && \text{at } r > r_p \end{aligned} \tag{11}$$

3 Solution of the consolidation equation around spherical cavity

The equations governing the consolidation of fully saturated porous elastic soil under one-dimensional may be attributed to Terzaghi (1923). These equations were extended by Biot (191) to cover the general three dimensional situations. Several modifications and developments have been made to the consolidation theories. A list of principal contributions to this subject can be found in Schiffman (1984), de Bore (2000), Schrefler(2002) and Selvadurai [12].

The relation between the variation of the volumetric strain v with time and the excess pore water pressure u_e around a spherical cavity can be expressed by:

$$\frac{\partial \varepsilon_v}{\partial t} = -\frac{k}{\gamma_w}\left[\frac{1}{r^2}\frac{\partial}{\partial r}\left(r^2\frac{\partial u_e}{\partial r}\right)\right] \tag{12}$$

where k is the permeability coefficient and γ_w is the unit weight of water.

For a linear elastic material we have:

$$\delta\varepsilon_v = \frac{3(1-2\nu)}{2G(1+\nu)}\delta p' \tag{13}$$

where v is the Poisson's ratio of the soil and G is the shear modulus, p' is the mean effective stress. If it is assumed that the total stresses remain constant during the consolidation, the change of the mean effective stress can be taken to be proportional to the change of excess pore water pressure. The mean effective stress decreases with the increase of pore water pressure. Eq. (12) can then be re-written as:

$$\frac{\partial u_e}{\partial t} = c\left(\frac{\partial^2 u_e}{\partial r^2} + \frac{2}{r}\frac{\partial u_e}{\partial r}\right) \tag{14}$$

where c is the coefficient of consolidation given by:

$$c = 2kG\frac{(1-\nu)}{(1-2\nu)\gamma_w} \tag{15}$$

where G is the shear modulus and ν is the Poisson's ratio.

If the coefficient of consolidation c is taken to be constant throughout the consolidation process, then Eq. (14) can be solved if the excess pore water pressure u_e can be expressed as a multiplication of two functions:

$$u_e = \xi(t)\cdot\psi(r) \tag{16}$$

Substituting in Eq. 14, gives:

$$\frac{1}{c\xi}\frac{\partial \xi}{\partial t} = \frac{1}{\psi}\nabla^2\psi \tag{17}$$

The left-hand side is now a function of t only and the right-hand side is a function of r, θ and ψ. Therefore equation 17 can be re-written as two separate equations:

$$\frac{1}{c\xi}\frac{\partial \xi}{\partial t} = -\lambda^2 \tag{18}$$

and

$$\frac{\partial^2 \psi}{\partial r^2} + \frac{2}{r}\frac{\partial \psi}{\partial r} + \lambda^2 \psi = 0 \tag{19}$$

where λ is a constant. The solution of Eq. (18) is given by:

$$\xi(t) = \exp(-c\lambda^2 t) \tag{20}$$

and the solution of Eq. (19) is a given by a combination of Bessel functions of the first and of the second kinds:

$$f_1(r) = \frac{A}{\sqrt{\lambda r}}\left[J_{1/2}(\lambda r) + \alpha Y_{1/2}(\lambda r)\right] \tag{21}$$

The full expression for u_e will involve a summation of all possible solutions:

$$u_e = \sum_{k=1}^{\infty} \frac{A_k}{\sqrt{(\lambda_k r)}}\left[J_{1/2}(\lambda_k r) + \alpha_k Y_{1/2}(\lambda_k r)\right]\exp(-c\lambda_k t) \tag{22}$$

where A_k, α_k, and λ_k are constants which are evaluated from the boundary conditions and J and Y are the Bessel functions of the first and second kind, respectively.

The boundary conditions around the spherical cavity are:

$$\begin{aligned}
u_e &= 0 && \text{at } r = \infty && (23)\\
\frac{\partial u_u}{\partial r} &= 0 && \text{at } r = r_0 \text{ for impermeable cavity} && (24)\\
u_e &= 0 && \text{at } r = r_0 \text{ for permeable cavity} && \\
u_e &= u_0 && \text{at } t = 0 && (25)
\end{aligned}$$

At some radial distance $R \gg r_0$, the excess pore pressure and the deformation are never more than negligibly small. Therefore, it could be assumed that $u_e = 0$ at $r = R$.

Satisfying the first boundary conditions in Eq. (23) implies that:

$$J_{1/2}(\lambda_k R) + \alpha_k Y_{1/2}(\lambda_k R) = 0 \tag{26}$$

so that the coefficients α_k are given by:

$$\alpha_k = -\frac{J_{1/2}(\lambda_k R)}{Y_{1/2}(\lambda_k R)} = \tan(\lambda_k R) \tag{27}$$

By substituting Eq.(27) in Eq. (24), the boundary condition given in Eq. 24 can be re-written as follows:

$$\begin{cases} \sin[\lambda_k(R-r_0)] & = 0 \qquad \text{for permeable cavity} \\ \sin[\lambda_k(R-r_0)] + \lambda_k r_0 \cos[\lambda_k(R-r_0)] & = 0 \qquad \text{for impermeable cavity} \end{cases} \tag{28}$$

where λ_k represent the non-zero roots. Thus, for a permeable cavity, we get:

$$\lambda_k = \frac{\pi k}{R-r_0} \tag{29}$$

Satisfying the first boundary conditions at $t = 0$ in Equation (25) implies that:

$$\sum_{k=1}^{\infty} \frac{A_k}{\sqrt{(\lambda_k r)}} \Big[J_{1/2}(\lambda_k r) + \alpha_k Y_{1/2}(\lambda_k r) \Big] = u_0 \tag{30}$$

Multiplying both sides of Equation (30) by $r^{3/2}[J_{1/2}(\lambda_k r) + \alpha_k Y_{1/2}(\lambda_k r)]$, integrating between r_0 and R and using the orthogonal properties of Bessel functions (McLachlan, 1957), gives:

$$A_k \int_{r_0}^{R} \frac{r}{\sqrt{\lambda_k}} \Big[J_{1/2}(\lambda_k r) + \alpha_k Y_{1/2}(\lambda_k r) \Big]^2 dr = \int_{r_0}^{R} u_0 r^{3/2} \Big[J_{1/2}(\lambda_k r) + \alpha_k Y_{1/2}(\lambda_k r) \Big] dr \tag{31}$$

Substituting the expression of u_0 from Eq. (11) and integrating both sides of Eq. (31), the values of A_k can then be found as follows:

$$A_k = \frac{\begin{gathered} Bs_u\sqrt{2\pi}\Bigg[[\sin(\lambda_k r_p)(1-\lambda_k r_p \tan(\lambda_k R)) - \cos(\lambda_k r_p)(\lambda_k r_p + \tan(\lambda_k R))] \\ -[\sin(\lambda_k r_0)(1-\lambda_k r_0 \tan(\lambda_k R)) - \cos(\lambda_k r_0)(\lambda_k r_0 + \tan(\lambda_k R))] \Bigg] \\ +4s_u\sqrt{2\pi}\Bigg[\cos(\lambda_k r_p)(\tan(\lambda_k R)) + \tan(\lambda_k R)\ln(r_p) + \lambda_k r_p \ln(r_0)) \\ -\sin(\lambda_k r_p)(1+\ln(r_p) + \lambda_k r_p \tan(\lambda_k R_0)\ln(r_p)) \\ +S_i(\lambda_k r_p) - C_i(\lambda_k r_p) \Bigg] \\ +4s_u\sqrt{2\pi}\Bigg[\cos(\lambda_k r_0)(\tan(\lambda_k R)) + \tan(\lambda_k R)\ln(r_0) + \lambda_k r_p \ln(r_0)) \\ -\sin(\lambda_k r_0)(1+\ln(r_0) + \lambda_k r_0 \tan(\lambda_k R_0)\ln(r_0)) \\ +S_i(\lambda_k r_0) - C_i(\lambda_k r_0) \Bigg] \end{gathered}}{\left[\dfrac{2\lambda_k(R-r_0) - \sin(\lambda_k(R-r_0))}{(1+\cos(2\lambda_k R))} \right]} \tag{32}$$

where B, $C_i(x)$ and $S_i(x)$ are given by:

$$B = \frac{4}{3} - N - 4\ln(r_0)$$
$$C_i(x) = -\int_x^\infty \frac{\cos(t)}{t}dt$$
$$S_i(x) = \int_0^x \frac{\sin(t)}{t}dt$$

4 Results and discussions

Fig.2 shows the variation of the excess pore water pressure with time for a point adjacent to impermeable cavity ($r = r_0$) for different values of stability numbers N. The excess pore water pressure normalized by undrained soil strength is calculated using Eq. 11. The normalized excess pore water pressure is plotted against the time factor T (Soderberg, 1962) defined as:

$$T = \frac{ct}{r_0} \tag{33}$$

The calculations are carried out assuming that the fixed-boundary of the soil deformation zone is located at R/r_0=60. A summation of 11268 terms of Eq. 22 was used. This number of terms corresponds to the number of nonzero roots λ_k of equation 30b for values of λr_0 between 0 and 600. This number of terms gives insignificant maximum error of 0.642% for N=2 for the value of the initial excess pore water pressure (at t=0 and $r = r0$) calculated using Eq. (11).

The analytical solution shows that the negative pore water pressure developed adjacent to the spherical cavity and its magnitude is proportional to the stability number. Negative excess pore pressure around tunnels is evident from field measurements (Palmer and Belshaw, 1980; Glossop, 1980; Shirlaw and Doran, 1988) and centrifuge data (Mair and Taylor, 1993).

Fig. 3 shows the isochrones of pore water pressure around impermeable spherical cavity. The results are shown for $N = 2$ and $N = 10$. The results show that development of pore water pressure is more localized around the tunnel in the case of $N = 2$ compared to $N = 10$. This is due to the fact that negative pore water pressure is resulted from the development of plastic zone around the tunnel. The extent of the plastic zone is proportional to the stability number N as illustrated from Eq. (9). The results shown in Fig. 3 also illustrates that the gradient of pore water pressure adjacent to the cavity contraction decreases with the consolidation time. Fig. 4 shows the isochrones adjacent to permeable spherical cavity.

5 Conclusion

A closed form solution for the variation of the excess pore water pressure with time around spherical cavity contraction was derived. The initial pore water pressure is evaluated from cavity contraction theory assuming the soil is elasto-perfectly plastic material. The variation of pore water pressure with time is established taking the soil to be a porous linear elastic material. In this solution, drainage is assumed to occur at the boundary of the assumed zone of deformable soil around the elastic sphere.

As demonstrated by Mair and Taylor (1993), the conditions around the tunnels can be simulated by cylindrical cavity and around tunnel heads can be simulated by spherical cavity. Therefore, this solution can be used to estimate initial pore water pressure during tunnel construction. It could also be used to variation of pore water pressure with time.

References

[1] Belshaw, D.J., Palmer, J.H.L., 1978. Results of a program of instrumention involving a precast segmented concretelined tunnel in clay. Canadian Geotechnical Journal. 15, 573-583.

[2] Biot, M.A., 1941. General theory of three-dimensional consolidation. Journal of Applied Physics. 12, 155-164.

[3] Carter, J.P., 1988. A semi-analytical solution for awelling around a borehole. International Journal for Numerical and Analytical Methods in Geomechanics, 1988; 12, 197-212.

[4] Cryer, C.W., 1963. A Comparison of the Three-Dimensional Consolidation Theories of Biot and Terzaghi. Quarterly Journal of Mechanics and Applied Mathematics, 16(4), 401-412.

[5] de Boer, R., 2000. Theory of Porous Media. Highlights in Historical development and Current State, Springer-Verlag, Berlin, Germany.

[6] Glossop, N.H., 1980. Ground defomation caused by tunnelling in soft ground at Grimsby. Internal Report. Department of Mining Engineering, University of Newcastle upon Tyne, Newcastle, UK.

[7] Mair, R.J., Taylor R.N., 1992. Predictions of clay behaviour around tunnels using plasticity solutions. In Proceedding of Predictive Soil Mechanics, Oxford, 449-463, London: Thomas Telford.

[8] McLachlan N.W., 1955. Bessel Functions for Engineers. Oxford, Clarendon Press, 2nd edition.

[9] de Josselin de Jong G., 1953. Consolidation around pore pressure meters. Journal of Applied Physics, 1953,24(7), 922-928.

[10] Schrefler, B.A., 2002. Mechanics and thermodynamics of saturated/unsaturated porous materials and quantitative solutions. Applied Mechanics Review, (55)4, 351-388.

[11] Scott, R.F., Radial consolidation of a phase-change soil. Geotechnqiue, 40(2), 211-221.

[12] Selvadurai, A.P.S., 2007. The analytical method in geomechanics. Applied Mechanics Reviews. 60(3), 87-106.

[13] Zhou, Y., Rajapakse, R.K.N.D., Graham, J., 1998. Coupled consolidation of a porous medium with a cylindrical or a spherical cavity. International Journal for Numerical and Analytical Methods in Geomechanics, 22(6), 449-475.

[14] Randolph, M.F., Wroth, C.P., 1978. An analytical solution for the consolidation around a driven pile. International Journal for Numerical and Analytical Methods in Geomechanics, 3, 217-229.

[15] Soderberg, O., 1962. Consolidation theory applied to foundation pile time effects. Geotechnique, 12(3), 217-225.

[16] Yu HS., Rowe RK. Plasticity solutions for soil behaviour around contracting cavities and tunnels. *Int. J. Numer. Anal. Meth. Geomech.*, 1999, **23**, 1245-1279.

[17] Yu HS., Houlsby GT. A Large Strain Analytical Solution for Contraction in Dilatant Soils. *Int. J. Numer. Anal. Meth. Geomech.*, 1995, **19**, 793-811.

[18] Terzaghi, K.Van. Die Berchnung der Durchassigkeitziffer des Tones aus dem Verlauf der Hydrodynamischen Spannungscheinungen. Sitzunzsber Akad Wiss.Wein Math Naturwiss, 1923, 107-122.

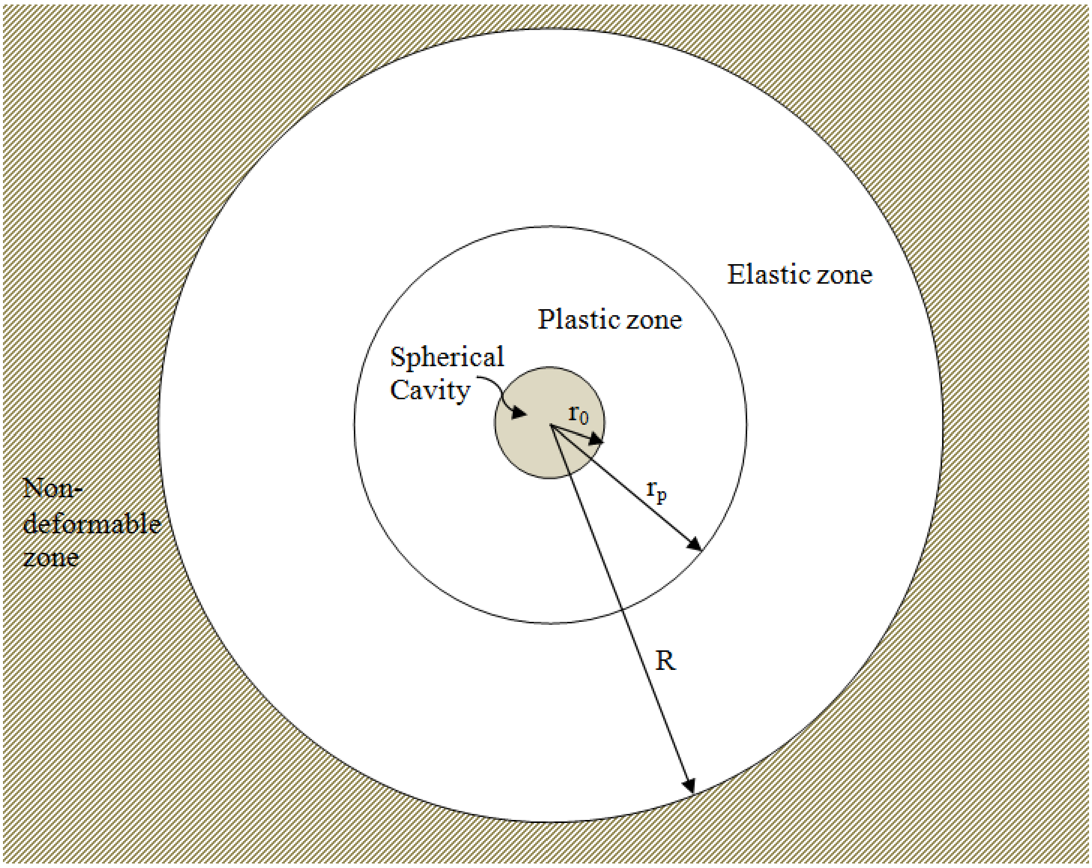

Figure 1: Schematic of cavity contraction problem.

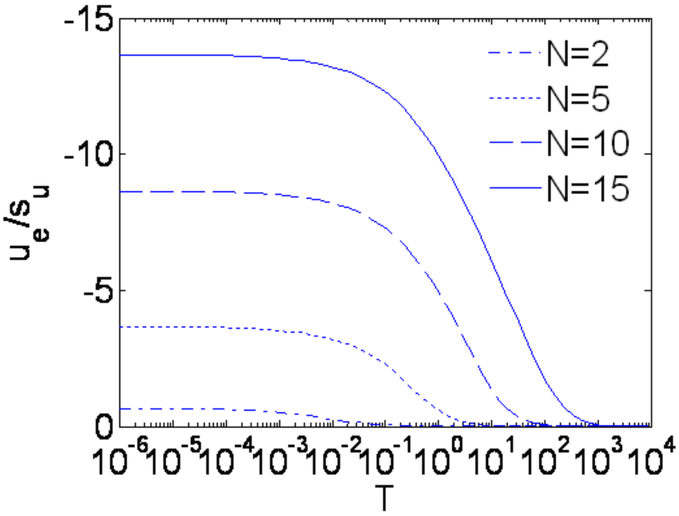

Figure 2: Variation of excess pore water pressure with time for a point adjacent to impermeable spherical cavity.

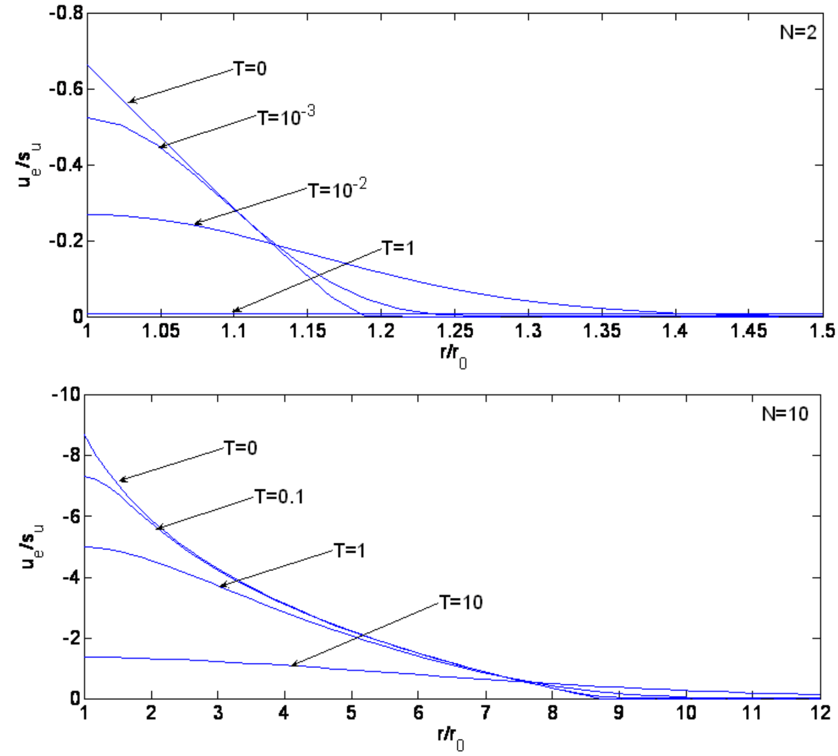

Figure 3: Isochrones of excess pore water pressure around impermeable cavity (a) N=2 and (b) N=10.

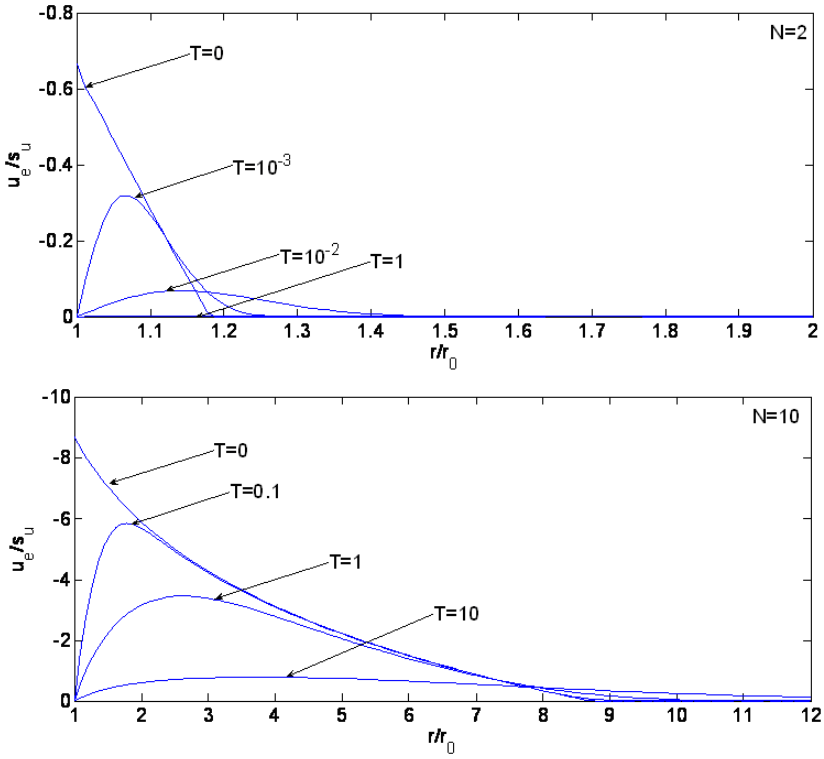

Figure 4: Isochrones of excess pore water pressure around permeable cavity (a) N=2 and (b) N=10.